

1 • Article type: paper

2 • 28th August 2014

3

4 Title

5

6 Is colour change a good measure of a water penetration front?

7

8

9 Author 1

10 • N. Fischer, engineering doctorate student

11 • HeidelbergCement Technology Center, Oberklamweg 6, 69181 Leimen,

12 Germany

13 • Micro and NanoMaterials and Technologies Industrial Doctorate Centre,

14 University of Surrey, Guildford, United Kingdom

15 Author 2

16 • R. Haerdtl, Dr-Ing.

17 • HeidelbergCement Technology Center, Oberklamweg 6, 69181 Leimen,

18 Germany

19 Author 3

20 • P. J. McDonald, Professor of Physics

21 • Department of Physics, University of Surrey, Guildford, Surrey, United

22 Kingdom

23

24

25 Corresponding author: P. J. McDonald, Department of Physics, University of
26 Surrey, Guildford, Surrey, GU2 7XH, United Kingdom p.mcdonald@surrey.ac.uk

27

28

29

30 Abstract

31 GARField nuclear magnetic resonance (NMR) profiling is used to
32 demonstrate that the sharp colour change boundary commonly used to locate
33 the water front in cement and concrete sorption tests is a poor indicator of the
34 true depth of water penetration. Across a range of mortars and concretes, NMR
35 invariably shows a smooth and often near zero gradient in the degree of
36 saturation at this boundary. Any sharp front that does exist, as might arise from a
37 strong dependence of the effective diffusivity on concentration and a multimodal
38 pore size distribution on the nanoscale is always far beyond the colour change
39 line.

40

41 Keywords

42 Sorption; NMR; Colour boundary;

43

44 List of notation

45 w/c water to cement ratio

46 r_K Kelvin-radius

47 ψ relative humidity

48 T temperature

49 M molar mass

50 σ surface tension

51 ρ density

52 θ contact angle between liquid and solid

53 R gas constant

54 T_2 nuclear spin-spin relaxation time

55

56 **1. Introduction**

57 Visual observation of a colour change at a water ingress front in
58 cementitious materials is a common method to determine water uptake in test
59 methods such as the sorptivity and the water penetration under pressure test
60 (BS EN 12390-8:2009).

61 Sorptivity is measured by capillary uptake and has units of distance per
62 root time: $m s^{-1/2}$. Sorptivity was first introduced by (Philip 1957) in the field of
63 hydrology. Hall (Hall 1977, Hall 1981) subsequently applied the term and test
64 procedure to cementitious materials. The test comprises of placing a pre-dried
65 sample above a water reservoir and watching the capillary uptake of water into
66 the porous structure. Either the increasing mass of the sample is measured at
67 intervals during the capillary uptake, or the sample is split and an internal
68 surface inspected for a visual water front. In the latter case, a plot of depth of
69 penetration against square root of time is expected to be a straight line for times
70 sufficiently short that the front does not approach the other end of the sample. It
71 has been noted before that the sorptivity derived from mass uptake and
72 penetration depth analyses usually differ (Basheer 2001). Moreover, in the case
73 of visual measurements, it has been suspected that some water ingresses beyond
74 the colour change front (Hall, Hoff 2009).

75 The water penetration under pressure test as a measure of permeability
76 was first introduced by (Murata 1965). Several mix designs, durations of test and
77 applied pressure were investigated. It was concluded that the water penetration
78 depth determined by visual observation was an appropriate method to measure
79 permeability. RILEM Recommendations (RILEM TC 1994) specified the area
80 where pressure is applied depending on sample size and also the applied
81 pressure steps and duration. The test procedure became standardised in
82 Germany in 1986 (DIN 1048:5 1991) and then used internationally (ISO/DIS
83 7031). These standards used a similar procedure to the technical
84 recommendation. The German standard later became the base for the current EN
85 12390-8 European standard.

86 The purpose of this short report is to present nuclear magnetic resonance
87 imaging (MRI) evidence that the colour change front can present a significantly

88 inaccurate measure of the actual water from position. Profiles of the water
89 concentration profile in mortar cylinders after 1 day of sorption obtained using a
90 laboratory GARField NMR system (Glover et al. 1999) are compared to
91 photographic recording of the colour-change front. Data sets show that the water
92 penetrated region extends well beyond that indicated by visual observation of
93 the colour boundary. Parallel measurements using a Surface Garfield NMR
94 system (McDonald et al. 2007) of the water sorption profile into the surface of
95 concrete blocks show similar effects. The temporal development of the water
96 concentration spatial profile, the water distribution within the open porosity,
97 and evidence for C-S-H swelling in the same materials are reported elsewhere
98 (Fischer et al 2014, Fischer 2014).

99

100 **2. Materials and Methods**

101

102 **2.1. Materials.**

103 Standard mortar(BS EN 196-1:2005) samples were mixed and cast into
104 cubic moulds of 150 mm side length. The mortar mix had a ratio of 0.5 : 1 : 3 by
105 mass for water : binder : aggregate. Two different binders were investigated,
106 Portland cement and Portland cement with 10 % silica fume by mass added at
107 mixing. One day after casting, the cubes were removed from the moulds and
108 further cured at 20°C for a minimum of 3 months either sealed in a double layer
109 of plastic sheet or underwater in lime water. One cube was prepared for each
110 mixture and curing method.

111 Cylinders of 18 mm diameter and 150 mm length were wet cored from
112 the cured cubes. The paste skin that forms on the surface of the sample at casting
113 was not removed from the end of the cylinders. The mortar cylinders were dried
114 to constant mass at 60°C, and under light vacuum to minimise carbonation, over
115 a period of about 2 weeks. After drying, the samples were wrapped with PTFE
116 tape with the two ends open.

117 The cylindrical samples were then exposed to liquid tap water from one
118 end. To do this, the cylinders were suspended above a shallow pool of water with

119 the lower end 1-2 mm below the water surface. The water level was kept
120 constant. The PTFE wrapping prevented drying from the sides and encouraged
121 one-dimensional water transport along the length of the cylinders. Other
122 common sealants and tapes, such as epoxy coating could not be used as they give
123 a significant ^1H background signal in NMR.

124 Concrete slabs were also investigated with the same binders and w/b
125 ratio. An example of a sealed cured OPC concrete and an OPC with 10% silica
126 fume are included in this report. The concrete slabs were cut from the centre of
127 the 150 mm cubes. Similarly to the mortars, the samples were dried to constant
128 mass at 60°C. After drying, the cut surface was stood in water for the uptake test.
129 The sides of the slabs where the colour-change water-front line was observed
130 had a thin paste skin originating from casting / curing. To ensure that this did
131 not significantly affect the results, a slab was split in half to observe the internal
132 water-front. It was found to be in good agreement with the surface.

133

134 **2.2. Methods**

135 Capillary water sorption was assessed in three ways: gravimetrically, by
136 observation (photographic recording) of the colour-change front and by ^1H
137 spatially localised NMR relaxometry. The sample mass was measured after 1, 2,
138 4, 8 and 24 hours of sorption. The purpose was to ensure that we remained in
139 the region of linear dependence of uptake on the square root of time. A
140 photograph of the sample with the same reference white background and scale
141 was taken after 24 hours of sorption. An NMR profile was also acquired after 24
142 hours of capillary sorption. In general, more frequent periodic recording was not
143 done, as this would have required overly exposing the sides of the sample to the
144 atmosphere. For NMR profiling, mortar cylinders were stepped through the
145 resonant plane of a laboratory GARField magnet. The step size was normally 1
146 mm. At each step, a Carl-Purcell-Meiboom-Gill (CPMG) echo train was recorded
147 (Meiboom, Gill 1958). The ^1H NMR frequency was 23.4 MHz and the $\pi/2$ pulse
148 length was 6.5 μs . A total of 64 echoes with 64 μs echo spacing and
149 2048 averages were recorded at each step.

150 A simple profile of the water content was constructed by summing the
151 echo intensities at each location. This yields a profile with a relatively good
152 signal-to-noise ratio. However, the echo-sum intensity is not linearly
153 proportional to water content. A better measure is provided by fitting the echo
154 train data to multi-exponential decays. It is well established that water in more
155 mobile environments / larger pores exhibits a longer decay time. To that end, the
156 first 2 echoes (that contain a significant contribution from the hydrate gel
157 interlayer water and that can suffer from artefact) were disregarded at each
158 location and the remainder fit to a two component exponential decay plus
159 baseline representing water in gel pores, interhydrate spaces and capillary pores
160 respectively (Muller et al 2013). The sum of these three amplitudes is thus a
161 measure of the evaporable water content. The baseline was used since the
162 maximum echo time (4.1 ms) was less than the expected decay time of capillary
163 water. Chemically combined water (in, e.g. Portlandite) has a decay time too
164 short for even the first echo.

165

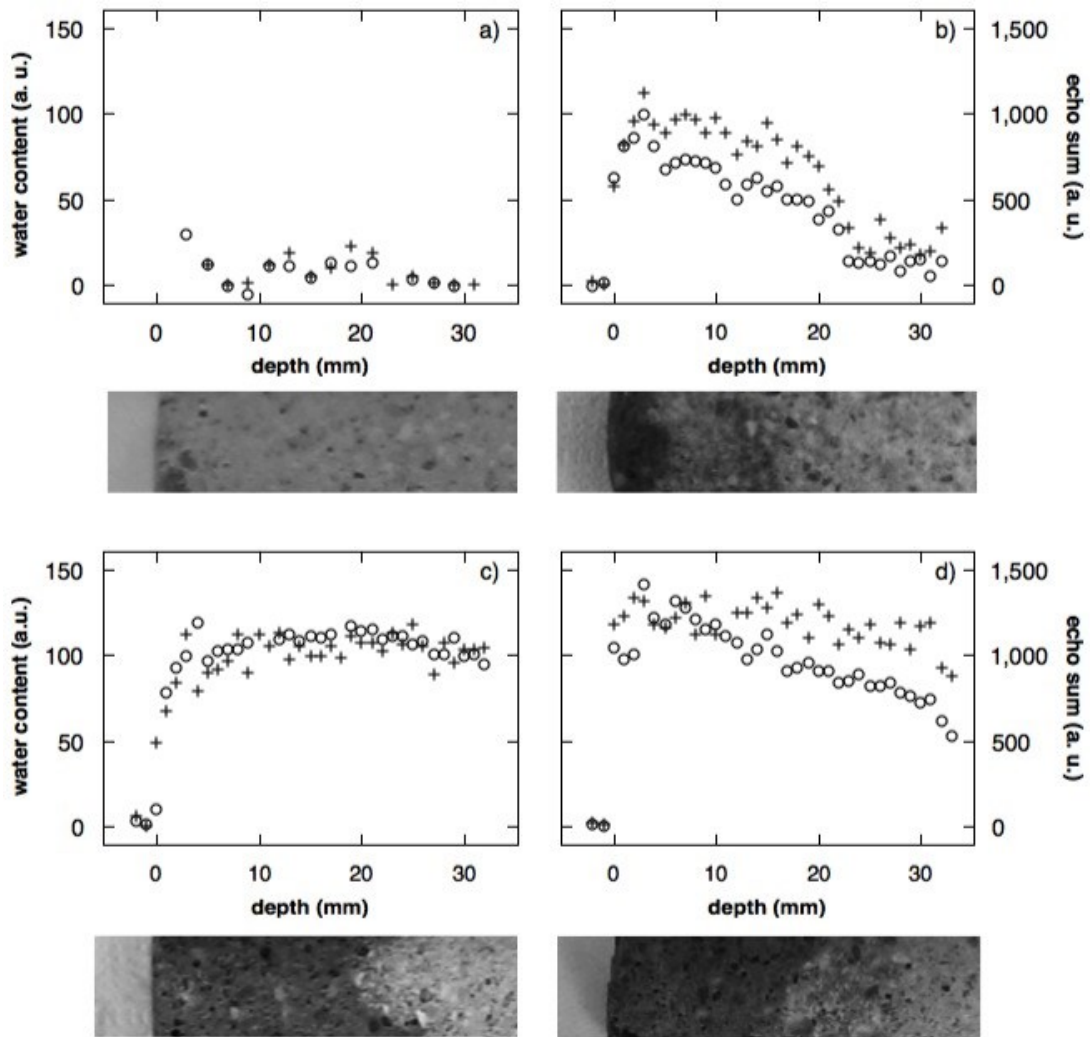
166 **3. Results and analysis**

167 Figure 1a and 1b show NMR profiles of water in the first 32 mm of sealed-
168 cured OPC-mortar cylinders after drying and again after 1 day of sorption
169 respectively. The exposed surface is at 0 mm on the scale. The profiles are
170 constructed in two ways: as echo sum data (right hand access) and from the total
171 amplitude of the exponential fits to the echo train data (left hand access).
172 Typically for the parameters used most of the signal occurs in the first 10-12
173 echoes. Hence the echo sum is about ten times the initial amplitude, though both
174 are of course in arbitrary units. The profiles show water invading about 22 mm
175 into the sample, with a sharp front at about 22 mm on the scale. The fact that the
176 pre-sorption intensity is close to baseline supports the claim that evaporable
177 water is being monitored. According to the echo sum data, there is a significant
178 gradient in concentration across the invaded region after 1 day of sorption.
179 However, this is much less evident in the intensity derived from the echo-train
180 fitting analysis. The difference likely reflects a redistribution of the water in the

181 nanoscale porosity due to C-S-H swelling that is discussed elsewhere (Fischer et
182 al 2014).

183 Photographs of the same section of the cylinder before and after sorption
184 are shown immediately below the profile plots. The photographs are all
185 greyscale and slightly enhanced for brightness. All photographs were taken with
186 the same white background. Before sorption, the dry sample is uniformly light
187 coloured. After 1 day of sorption there is a clear darkening of the wetted surface
188 layers with a clear colour boundary at about 5 mm. Beyond this the sample is
189 slightly darker and there is an indication a weaker colour change at about 14
190 mm. However, whichever boundary is taken as the water front, neither extends
191 as far as the NMR shows water to penetrate.

192 Figure 1c and 1d repeat figure 1b for two further samples of the same
193 mortar. In these samples, the water travels much further in one day by both
194 measures. The visual interface is much more evident in these samples and so the
195 results are even less ambiguous. The NMR profile shows greater ingress than the
196 optical measurement in each case. Indeed, in the case of 1b water extends
197 beyond 32 mm. The water concentration measured by NMR is relatively smooth
198 across the visual interface. However, careful observation suggests that there is a
199 slight change in gradient at the colour change, notably for the echo sum data.
200 Echo sum has the effect of magnifying the contribution of water content in larger
201 capillary pores relative to smaller gel pores. A key question is why the sorption
202 in figure 1b is substantially less than in figure 1c or 1d. The answer lies in the
203 sample history. The sample used for figure 1b was cast in May, cured sealed,
204 cored and dried in August and used for sorptivity in January. Those for figures 1c
205 and 1d were cast in May (same cube) cored and dried in January and used for
206 sorptivity in February.

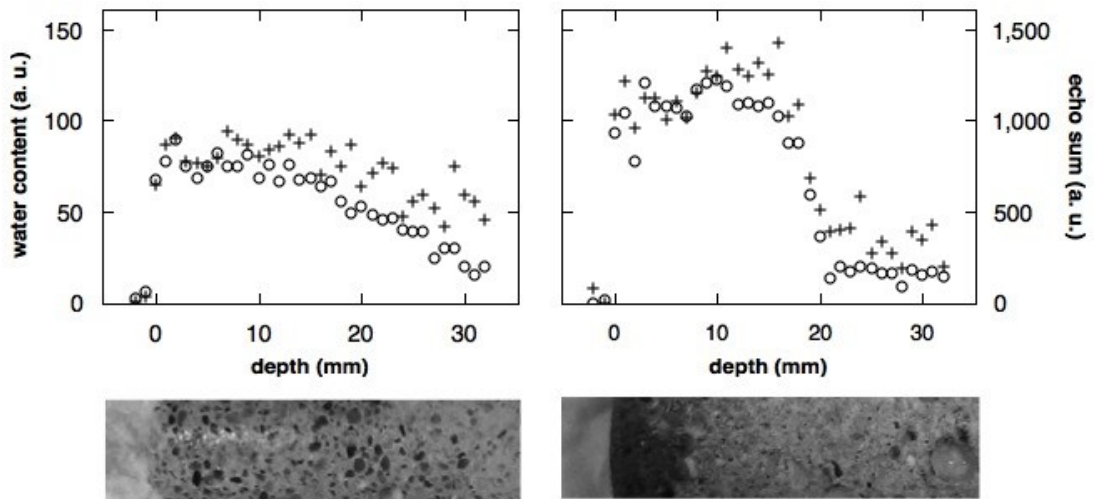


207

208 Fig 1. NMR profiles and photographs of a sealed cured OPC mortar
 209 cylinder use in sorption experiments: (a) dry and (b) after 1 day of capillary
 210 sorption. The profiles are constructed from echo sums (circles, right hand axes)
 211 and exponential fitting intensities (crosses, left hand axes). (c) and (d) are
 212 profiles and photographs of 2 further samples after 1 day of sorption. All
 213 cylinders were cored from the same cube of mortar. The cylinder used in (a and
 214 b) was dried 4 months before use. The cylinders in (c and d) were not dried until
 215 needed.

216 Figure 2 shows examples of an underwater cured OPC mortar and a
 217 sealed cured OPC mortar with silica fume after 1 day of capillary sorption. In
 218 case of the underwater cured sample, the wet region is less marked in the
 219 photographs. Notwithstanding, a weak colour change boundary can be discerned

220 at about 22 mm on the scale. The NMR profile constructed from the echo sum
 221 shows a gradual water concentration gradient right across this boundary. The
 222 profile constructed from the fitted echo amplitude is more constant around 22
 223 mm with a more marked interface nearer 30 mm. In the case of the sample with
 224 silica fume, the water front is much more marked, both optically and by NMR.
 225 However, the former is at about 6 mm depth, whereas the latter is at about 18
 226 mm.



227

228 Fig 2. Under water cured OPC mortar (left) and sealed cured OPC with
 229 silica fume mortar (right) sample after 1 day of sorption. NMR profile of
 230 gel+capillary water (crosses, left axes) and echo sum (circles, right axes).
 231 Photographs of the same area are below the NMR data

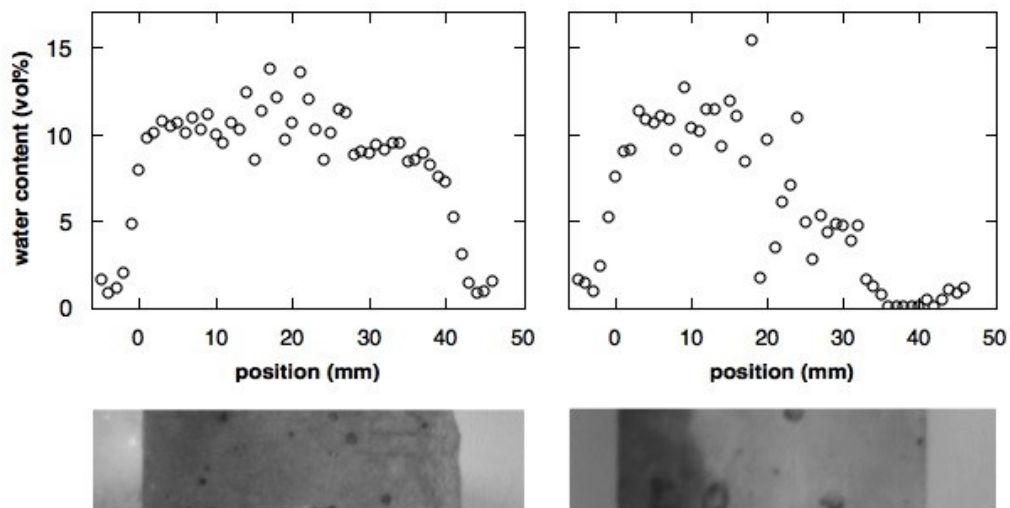
232

233 In total, 4 sealed and 2 underwater cured OPC mortars and 3 sealed cured
 234 OPC mortars with silica fume were investigated. In every case the water ingress
 235 as measured by NMR profiling extended significantly beyond the water front
 236 indicated by the colour change boundary. In no case, was there an unambiguous
 237 sharp feature in the NMR data at the colour change boundary.

238

239 Figure 3 shows two concrete samples measured by the surface GARField.
 240 The signal to noise ratio decreases with depth with surface GARField. The
 241 profiles shown are constructed from measurements from both sides of the

242 sample. Hence the signal to noise ratio of the data is worst in the profile centre.
 243 The profiles are shown as echo sums only as the signal to noise ratio in these
 244 measurements did not permit exponential fitting. The surface in contact with
 245 water is at 0 mm. The photographs of the cross section of the samples are below
 246 the NMR profiles. In case of the OPC concrete, the sample was wet all the way
 247 through as measured by NMR. However, the photograph shows a gradual colour
 248 change boundary nearer 15 mm. The first 15 mm from the left side is darker
 249 than the rest of the sample. In the case of the OPC concrete with silica fume there
 250 is an even more clear water line, about 10 mm from the wet surface. However,
 251 the NMR profile shows water extending well beyond this dark region, down to
 252 about 30 mm from the wet surface.



253
 254 Fig 3. Echo sum NMR profiles concrete samples after 1 day of sorption
 255 with photographic cross-sections below. The samples are sealed cured OPC
 256 concrete (left) and OPC concrete with silica fume (right).

257

258 4. Discussion

259 In a capillary uptake experiment, there is a gradient of internal relative humidity
 260 in the sample from 100% where the sample is in contact with liquid water down
 261 to the ambient value at the exposed end. Capillary uptake of water at the lower
 262 end, evaporation at the water front, and a detailed liquid and vapour mass flow

263 rate balance though pore network lead to a non-uniform water content profile as
264 has been discussed by Hall and Hoff (Hall, Hoff 2009).

265 Theoretical understanding of the colour change of wetted porous ceramic bricks
266 has been discussed previously (Hall, Hoff 2009). It is a complex problem. Not
267 withstanding, it is reasonable to assume that the colour change is associated with
268 the wetting of pores of size comparable to the wavelength of light, circa 400-700
269 nm. The Kelvin equation

270
$$r_K = -\frac{2\sigma M \cos \theta}{RT\rho \ln \psi}$$

271 gives the critical radius, r_K , of a pore that is filled with water at a relative
272 humidity, ψ , and temperature, T . In this equation M is the molar mass, σ the
273 surface tension, ρ the density and θ the contact angle of the liquid in the pore and
274 R is the gas constant. For optical wavelengths, and using parameters for water
275 and assuming that water wets cement, this suggests that the colour change
276 occurs at relative humidities exceeding 99.7 %.

277 The NMR signal lifetime, (the nuclear spin-spin relaxation time, T_2) of ^1H in
278 water in small pores is proportional to the pore size (D'Orazio et al. 1990). The
279 NMR measurements made in this work are sensitive to water in gel pores (a few
280 nanometres), inter-hydrate pores (a few tens of nm) and larger capillary pores
281 (100 nm to mm) resultant from chemical shrinkage and air voids in the original
282 mix (Muller et al. 2013). By the Kelvin equation, and taking representative sizes
283 of 3, 30, 300 and 3000 nm, these different pore sizes fill at relative humidities of
284 70, 96, 99.6% and >99.9%. There is inevitably a (non-constant) gradient in
285 vapour pressure across the sample during sorption: the upper face of the sample
286 is in equilibrium with the atmosphere. Given that the NMR senses water across a
287 very wide range of pore sizes, and hence relative humidities, it is therefore
288 reasonable to expect that water is seen over a great spatial range. One does not
289 then expect to see a sharp feature in the NMR water profile at the colour change
290 boundary. Such sharp boundaries as do occur are beyond this line and could well
291 be associated with the multi-modal pore size distribution on the nano-scale as
292 revealed by NMR (Muller et al. 2013).

293

294 **5. Conclusions**

295 A colour change boundary line is often used to determine the penetration
296 water front in cement and concrete water transport test procedures. The results
297 should be treated with caution. NMR profiling yields clear evidence that there is
298 significant amount of water beyond the colour change line in sorptivity tests. In
299 most cases, the degree of saturation of the sample is only marginally less beyond
300 the darkened region and there is, in general, no marked change in the degree of
301 saturation gradient as this boundary is crossed. Notwithstanding, in many
302 instances there is a sharp water front as predicted by several numerical models
303 on the basis of a strong dependence of the effective diffusivity on pore size and
304 vapour pressure and hence saturation. However, as shown by NMR, it occurs
305 significantly beyond the optical boundary.

306 The results in this paper focused on water ingress into dried material. The
307 water penetration under pressure test focuses on water ingress into already wet
308 material. This test also relies on visual observation. Other experiments to be
309 reported elsewhere (Fischer 2014) show that NMR does not detect a strong front
310 under those conditions either.

311

312 **Acknowledgements**

313 The research leading to these results has received funding from the
314 European Union Seventh Framework Programme (FP7/2007-2013) under grant
315 agreement 264448

316

317 **References**

318 Basheer, P.A.M. 2001, "16 - Permeation Analysis" in *Handbook of Analytical*
319 *Techniques in Concrete Science and Technology*, eds. V.S. Ramachandran & J.J.
320 Beaudoin, William Andrew Publishing, Norwich, NY, pp. 658-737.

321 BS EN 12390-8:2009 *Testing hardened concrete - Part 8: Depth of penetration of*
322 *water under pressure.*

323 BS EN 196-1:2005 *Methods of testing cement. Determination of strength.*

- 324 DIN 1048:5 1991, *Prüfverfahren für Beton; Festbeton, gesonderd hergestellte*
325 *Probekörper.*
- 326 D'Orazio, F., Bhattacharja, S., Halperin, W.P., Eguchi, K. & Mizusaki, T. 1990,
327 "Molecular diffusion and nuclear-magnetic-resonance relaxation of water in
328 unsaturated porous silica glass", *Physical Review B*, vol. 42, no. 16, pp. 9810-
329 9818.
- 330 Fischer, N. 2014, *Validation of conventional water transport test methods by*
331 *spatially resolved ¹H magnetic resonance*, EngD thesis, University of Surrey,
332 (in preparation).
- 333 Fischer, N., Haerdtl, R. & McDonald, P.J. 2014, "Observation of the redistribution
334 of nanoscale water filled porosity in cement based materials during wetting"
335 Cement and Concrete Research (submitted)
- 336 Glover, P. M., Aptaker, P.S., Bowler J.R., Ciampi, E. and McDonald P.J., 1999 "A
337 novel high gradient permanent magnet for the imaging of planar thin films",
338 *Journal of Magnetic Resonance*. vol. 139, no 1, pp. 90-97.
- 339 Hall, C. & Hoff, W.D. 2009, *Water Transport in Brick, Stone, and Concrete*, 2nd edn,
340 Spon Press.
- 341 Hall, C. 1981, "Water movement in porous building materials—IV. The initial
342 surface absorption and the sorptivity", *Building and Environment*, vol. 16, no.
343 3, pp. 201-207.
- 344 Hall, C. 1977, "Water movement in porous building materials—I. Unsaturated
345 flow theory and its applications", *Building and Environment*, vol. 12, no. 2,
346 pp. 117-125.
- 347 ISO/DIS 7031 "Concrete hardened - Determination of the depth of penetration of
348 water under pressure", .
- 349 McDonald, P.J., Aptaker, P.S., Mitchell, J. & Mulheron, M. 2007, "A unilateral NMR
350 magnet for sub-structure analysis in the built environment: The Surface
351 GARField", *Journal of Magnetic Resonance*, vol. 185, no. 1, pp. 1-11.
- 352 Meiboom, S. & Gill, D. 1958, "Modified spin-echo method for measuring nuclear
353 relaxation times", *Review of Scientific Instruments*, vol. 29, no. 8, pp. 688-691.
- 354 Muller, A.C.A., Scrivener, K.L., Gajewicz, A.M. & McDonald, P.J. 2013,
355 "Densification of C-S-H Measured by ¹H NMR Relaxometry", *The Journal of*
356 *Physical Chemistry C*, vol. 117, no. 1, pp. 403-412.
- 357 Murata, J. 1965, "Studies on the Permeability of Concrete", *Materials and*
358 *Structures*, , no. 29, pp. 47-54.

- 359 Philip, J.R. 1957, "The Theory of Infiltration: 4. Soprtivity and Algebraic
360 Infiltration Equations", *Soil Science*, vol. 84, no. 3, pp. 257-264.
- 361 RILEM TC 1994, "CPC 13.1 Teste for the penetration of water under pressure on
362 hardened concrete, 1979" in *RILEM Recommendation for the Testing and Use
363 of Construction Materials*, ed. RILEM, E & FN SPON, , pp. 41-42.
- 364